

Task-Adaptive Physical Reservoir Computing via Tunable Molecular Communication Dynamics

Saad Yousuf, Kaan Burak Ikiz, and Murat Kuscu

Nano/Bio/Physical Information and Communications Laboratory (CALICO Lab)

Department of Electrical and Electronics Engineering, Koç University, Istanbul, 34450, Turkey

{syousuf24, kikiz22, mkuscu}@ku.edu.tr

Abstract—Physical Reservoir Computing (PRC) offers an efficient paradigm for processing temporal data, yet most physical implementations are static, limiting their performance to a narrow range of tasks. In this work, we demonstrate *in silico* that a canonical Molecular Communication (MC) channel can function as a highly versatile and *task-adaptive* PRC whose computational properties are reconfigurable. Using a dual-simulation approach—a computationally efficient deterministic mean-field model and a high-fidelity particle-based stochastic model (Smoldyn)—we show that tuning the channel’s underlying biophysical parameters, such as ligand-receptor kinetics and diffusion dynamics, allows the reservoir to be optimized for distinct classes of computation. We employ Bayesian optimization to efficiently navigate this high-dimensional parameter space, identifying discrete operational regimes. Our results reveal a clear trade-off: parameter sets rich in channel memory excel at chaotic time-series forecasting tasks (e.g., Mackey Glass), while regimes that promote strong receptor nonlinearity are superior for nonlinear data transformation. We further demonstrate that post-processing methods improve the performance of the stochastic reservoir by mitigating intrinsic molecular noise. These findings establish the MC channel not merely as a computational substrate, but as a design blueprint for tunable, bioinspired computing systems, providing a clear optimization framework for future wetware AI implementations.

Index Terms—Molecular Communication, Task-Adaptive Computing, Physical Reservoir Computing, Bayesian Optimization, Wetware Computing, Ligand-Receptor Interactions.

I. INTRODUCTION

Physical Reservoir Computing (PRC) offers an efficient, low-power paradigm for temporal data processing by harnessing the dynamics of physical systems [1], [2]. However, most physical reservoirs are static, fixed by their construction. This inherent rigidity often results in a PRC that excels at one class of tasks but performs poorly on others, lacking the reconfigurability of software-based models [1]. The recent development of a task-adaptive PRC using a chiral magnet highlights the critical need for systems with tunable dynamics, where different computational tasks can be optimized by reconfiguring the system’s physical properties [3].

Our recent work introduced a new perspective by framing a canonical Molecular Communication (MC) channel as a PRC [Fig.1], demonstrating its inherent capability for complex temporal information processing [4], [5]. Building on this, we now demonstrate that a canonical MC channel can serve as a powerful, reconfigurable PRC *in silico*. We posit that the biophysical parameters governing the MC channel can act as

“control knobs” to deliberately tune the balance between its fading memory and nonlinearity, thereby adapting the reservoir for distinct computational objectives.

In this work, we establish the MC channel as a biophysically tunable PRC, creating a direct link between its physical parameters and computational capabilities. Using a dual-simulation framework, we demonstrate that the MC-reservoir can be optimized for fundamentally different classes of computation: a memory-dominant regime for chaotic time-series forecasting and a nonlinearity-dominant regime for nonlinear data transformation [6], [7]. To navigate the complex parameter space, we introduce an optimization framework based on Bayesian search, providing a computational blueprint for designing and tuning future “wetware” AI systems [8]–[10].

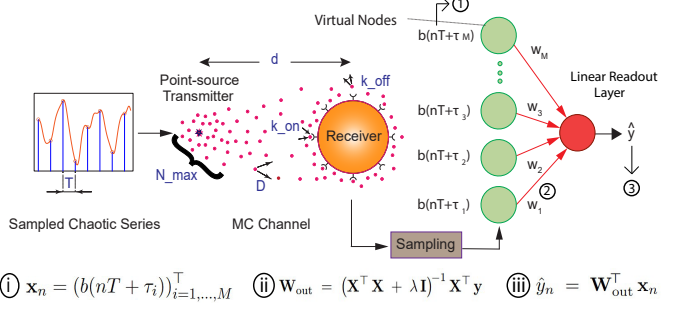


Fig. 1. Conceptual framework of the task-adaptive MC-PRC. The diagram illustrates the MC channel (transmitter, diffusion, receiver) with labels for the “Biophysical Control Knobs” (D , d , k_{on} , etc.). Three equations are labeled and shown to explain the mechanism of the PRC which are analyzed further in Section 2A.

We rigorously test these computational classes using specific benchmark tasks: **Mackey-Glass time-series forecasting**, a **Sine-to-Square wave transformation**, and a more complex **cubed Mackey-Glass** series that requires both memory and nonlinearity. Our findings validate this approach by identifying distinct, task-optimized clusters of biophysical parameters. We reveal a clear trade-off where, for instance, memory-intensive tasks favor parameters that maximize Inter-Symbol Interference (ISI), while nonlinear tasks benefit from parameters that drive the receiver into saturation, confirming that performance hinges on finely tuning these competing physical dynamics.

II. THE MC RESERVOIR COMPUTING FRAMEWORK

We consider a single-link MC system composed of a point transmitter and a spherical receiver, as detailed in our foundational work [4] [Fig.1]. We reframe this communication system as a PRC, where the biophysical dynamics inherent to the channel are not treated as impairments but are instead harnessed for computation. The input relevant to the computational task is fed into the reservoir at each discrete time step n is a scalar value $u(n)$, which is encoded into the number of molecules released by the transmitter.

A. System Model

The physical foundation of the MC-PRC lies in two key delay-based processes: molecular diffusion in the channel and ligand-receptor binding at the receiver. The propagation of ligands in the 3D fluidic medium is governed by Fick's second law of diffusion:

$$\frac{\partial c(\mathbf{r}, t)}{\partial t} = D \nabla^2 c(\mathbf{r}, t), \quad (1)$$

where D is the diffusion coefficient and $c(\mathbf{r}, t)$ is the ligand concentration at position \mathbf{r} and time t . The slow nature of diffusion causes transmitted molecular pulses to spread over time, resulting in a time-varying concentration profile at the receiver, $c_R(t)$, whose full analytical form is:

$$c_R(t) = \sum_{n=0}^{\infty} \alpha u(n) h(t - nT), \quad (2)$$

also explained in [4, Eq.5]. The term α is a scaling factor and the term $h(t)$ represents the channel's impulse response, which corresponds to the time-varying concentration profile at the receiver resulting from a single, instantaneous molecular emission at the transmitter. This temporal dispersion creates significant ISI, a phenomenon that provides a natural and rich source of fading memory for the reservoir, allowing it to retain information from past inputs.

At the receiver surface, the arriving ligands drive the state of the reservoir through reversible binding to receptors. The time evolution of the mean fraction of bound receptors, $b(t)$, which represents the continuous-time output of the reservoir, is modeled by first-order kinetics [11]:

$$\frac{db(t)}{dt} = k_{\text{on}} c_R(t) [1 - b(t)] - k_{\text{off}} b(t). \quad (3)$$

The $k_{\text{on}}, k_{\text{off}}$ terms refer to the binding and unbinding rate constants of the receptors, while the saturating term $[1 - b(t)]$ provides the essential nonlinearity for the reservoir's computational capability. As more receptors become occupied, the system's response to additional ligands diminishes, allowing for complex, nonlinear transformations of the input signal.

To form a high-dimensional state vector required for PRC, the continuous-time signal $b(t)$ is processed through time-multiplexing. As illustrated in a representative trace, $b(t)$ is sampled at M distinct time offsets within each symbol interval. These samples act as "virtual nodes," and their collective values form the reservoir state vector $\mathbf{x}_n \in \mathbb{R}^M$ for the

input $u(n)$ [12]. The specific construction of this state vector, by sampling the continuous-time signal $b(t)$ at various delay times, is shown in [Fig.1, Eq.(i)].

This high-dimensional state vector is then processed by a linear readout layer, which is trained to map the reservoir's complex dynamics to a desired output. The final prediction, \hat{y}_n , is computed as a weighted sum of the reservoir state components, as shown in [Fig.1, Eq.(iii)]. The key to the PRC's performance lies in optimizing the readout weights, \mathbf{W}_{out} , during a supervised training phase. The closed form solution is given by the Moore-Penrose pseudoinverse, shown in [Fig.1, Eq.(ii)]. This training process effectively learns to extract the relevant features encoded in the reservoir states for the specific task at hand. This process effectively maps the low-dimensional input history onto a high-dimensional state space, where complex relationships can be linearly separated.

In summary, the MC channel itself functions as the physical reservoir. The interplay between the ISI-induced memory from diffusion and the saturation-induced nonlinearity from receptor kinetics provides the necessary ingredients for powerful temporal computation. The characteristics of these dynamics are dictated by the underlying biophysical parameters of the system, which, as we show, can be tuned to reconfigure the reservoir for different tasks.

B. Reconfigurable Biophysical Parameters

The key to task-adaptability in our MC-PRC lies in its biophysical parameters, which act as control knobs to tune the reservoir's dynamics. In this work, we demonstrate this principle *in silico* by systematically varying these parameters within physically realistic intervals to find optimized operational regimes for the task at hand. The main parameters that shape the reservoir's computational properties are as follows:

- **Receiver Kinetics** ($k_{\text{on}}, k_{\text{off}}$): The association (k_{on}) and dissociation (k_{off}) rate constants dictate the receiver's sensitivity and memory retention. The ratio $K_D = k_{\text{off}}/k_{\text{on}}$ determines the binding affinity. A low affinity (high k_{off}) results in a short-term memory as ligands unbind quickly, while a high affinity (low k_{off}) creates a longer memory but increases the risk of receptor saturation, which can diminish computational performance if not properly optimized.
- **Channel Propagation** (D, d): The diffusion coefficient (D) and the transmitter-receiver distance (d) collectively shape the channel's impulse response. A lower diffusion coefficient or a longer distance increases the temporal spread of molecular signals, thereby lengthening the ISI-induced fading memory of the reservoir. Conversely, a higher diffusion coefficient or shorter distance provides a shorter memory, which can be advantageous for tasks requiring rapid responses.
- **Signal Encoding** (N_{max}, T): The number of molecules released per pulse (N_{max}) and the symbol duration (T) directly control the input signal's characteristics. Increasing N_{max} boosts the signal strength, driving the receiver further into its nonlinear regime. Modulating T alters the

degree of ISI, directly influencing the amount of memory carried between consecutive inputs.

Our methodology uses this parametric control to find optimal system configurations for specific computational goals. By employing Bayesian optimization, we can efficiently search the high-dimensional space defined by these parameters to identify distinct regimes where the reservoir is either memory-dominant or nonlinearity-dominant. These parameters were varied within physically plausible ranges selected to be representative of typical biological and nanoscale systems as reported in the MC literature [9]. Although we demonstrate this framework on forecasting and nonlinear transformation tasks, the optimization method is general and can be applied to discover tailored configurations for any specific task.

Furthermore, it is important to note that this optimization is not solely an offline design choice. Many of these parameters possess the potential for online tuning in future physical implementations. For example, recent work has proposed methods for creating adaptive MC receivers where ligand-receptor interactions can be dynamically modulated [8]. Similarly, signal encoding parameters are adjustable at the transmitter. This suggests a clear pathway toward creating truly adaptive “wetware” computing systems that can reconfigure their physical dynamics in response to changing tasks or environments.

C. Tasks, Performance Metric, and Optimization

We evaluate the reconfigurable performance of the MC-PRC on three distinct classes of computational tasks. These tasks are specifically chosen to probe the fundamental trade-off between the reservoir’s memory and its nonlinear processing capabilities, inspired by standard RC benchmarks [13].

1) *Forecasting Task*: This task tests the reservoir’s ability to predict the future evolution of a chaotic time-series, a benchmark known to require significant and well-structured fading memory. We use the **Mackey-Glass series**, which is generated by the following time-delayed differential equation:

$$\frac{dx(t)}{dt} = \frac{\beta x(t - \tau)}{1 + x(t - \tau)^n} - \gamma x(t) \quad (4)$$

For our simulations, we use the standard parameters ($\beta = 0.2$, $\gamma = 0.1$, $n = 10$, $\tau = 17$) that produce chaotic behavior. The input to the reservoir is the value of the series at time t , $u(n) = x(t)$, and the objective is to predict the value at a future time, $y(t) = x(t + P)$. Success in this task hinges on the reservoir’s capacity to learn the intricate, long-term dependencies of the chaotic system, a memory-intensive process.

2) *Nonlinear Transformation Task*: This task mainly demands strong nonlinear mapping capabilities to transform an input waveform into a structurally different target, with less emphasis on long-term memory. Inspired by the benchmarks in [3], we use the **Sine-to-Square Transformation**, where the reservoir is fed a simple sine wave as input and must learn the highly nonlinear mapping required to convert it into a square wave of the same fundamental frequency.

3) *Combination Task*: To evaluate performance on a task that requires a sophisticated balance of both memory and nonlinearity, we use a **modified Mackey-Glass Series**, also inspired by [3]. The standard Mackey-Glass series is a benchmark for chaotic time-series prediction. For our purposes, we use the output of this series and cube it, creating a target signal $y(t) = x_{\text{MG}}(t)^3$. This modification introduces a strong nonlinear component to a task that is already memory-dependent, presenting a significant computational challenge.

4) *Performance Metric*: For all tasks, the prediction and transformation accuracy is quantified using the Normalized Root Mean Square Error (NRMSE), a standard metric in reservoir computing [13] defined as:

$$\text{NRMSE} = \sqrt{\left(\sum_{k=1}^{N_{\text{test}}} (y_k - \hat{y}_k)^2 \right) / \left(\sum_{k=1}^{N_{\text{test}}} (y_k - \bar{y})^2 \right)} \quad (5)$$

where y_k is the true target value, \hat{y}_k is the reservoir’s prediction, and \bar{y} is the mean of the true target values over the test set of size N_{test} . The NRMSE uses normalized error, providing a scale-independent measure of performance where lower values indicate higher accuracy.

5) *Hyperparameter Optimization*: To identify the optimal biophysical parameter sets for each distinct task, we employ **Bayesian optimization**. This methodology is exceptionally well-suited for our problem for two main reasons [10]:

- 1) The objective function (a full run of the MC-PRC simulation to calculate NRMSE) is computationally **expensive to evaluate**.
- 2) The parameter space is **high-dimensional**, consisting of seven distinct physical and sampling parameters.

A traditional grid search would be computationally prohibitive. Bayesian optimization, by contrast, intelligently explores the parameter space to find the optimum in far fewer evaluations, which is particularly effective for tuning complex machine learning systems [10], [14]. The process works by building a probabilistic model of the objective function and using that model to select the most promising parameters to evaluate next. The core components are:

- **A Surrogate Model**: A probabilistic model that approximates the true objective function. We use a **Gaussian Process (GP)**, which models our objective function $f(\mathbf{x})$ as a distribution over functions. A GP is defined by a mean function $\mu(\mathbf{x})$ and a covariance (or kernel) function $k(\mathbf{x}, \mathbf{x}')$, which captures the similarity between different parameter sets. The key advantage is that the GP provides not only a mean prediction of the NRMSE for a given parameter set \mathbf{x} but also the uncertainty (variance $\sigma^2(\mathbf{x})$) in that prediction.
- **An Acquisition Function**: An algorithm that uses the surrogate model’s predictions to decide which parameter set \mathbf{x} to evaluate next. It balances *exploitation* (sampling in regions where the model predicts a low NRMSE) with *exploration* (sampling where the model is highly uncertain). We use the **Expected Improvement (EI)**

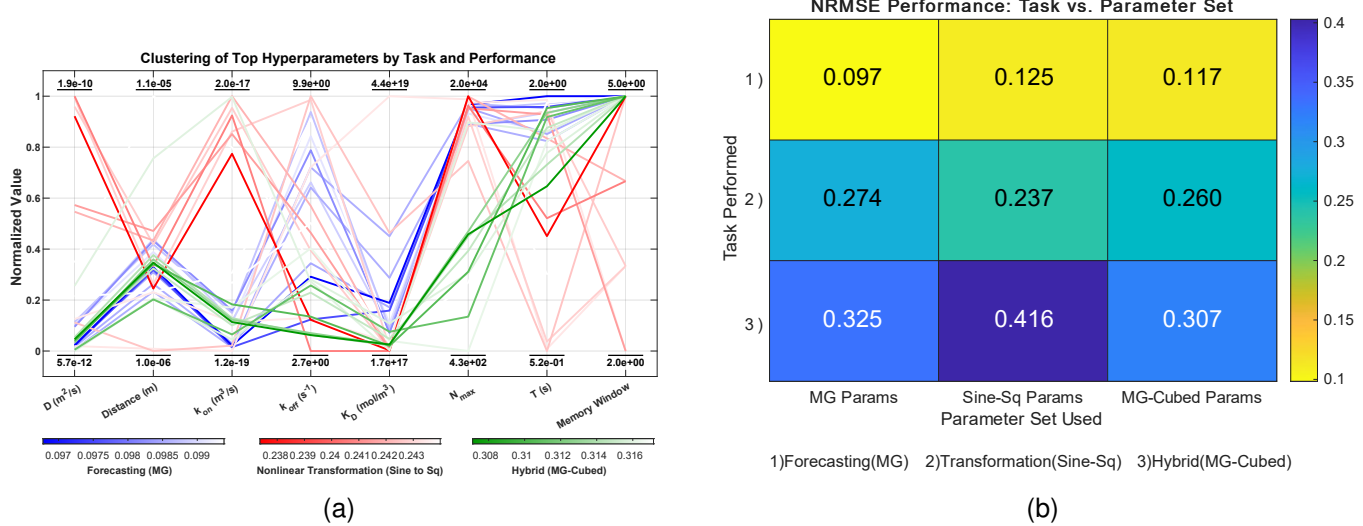


Fig. 2. **a) Task-Specific Clustering of Optimal Biophysical Parameters.** A parallel coordinates plot visualizing the top 10 best-performing parameter sets discovered by Bayesian optimization(200 deterministic model trials) for each of the three computational tasks. Each colored line represents a single, complete parameter set. The vertical axes correspond to the seven(also K_D , defined as k_{off}/k_{on}) biophysical parameters that were optimized. Clustering patterns emerge between the Forecasting task (blue), the Transformation task (red) and the Hybrid task (green). This visualization provides strong insight for the possibility of distinct, task-adaptive operational regimes in the MC-PRC. The “Memory Window Length” refers to a readout hyperparameter, included in the optimization, defining the number of recent reservoir states used for prediction. **b) Demonstration of task-adaptability through performance comparison.** The chart shows the NRMSE error for three distinct computational tasks on deterministic model when performed with parameter sets optimized for each specific task. The lowest error for each task is achieved only when using its corresponding matched parameter set, visually confirming that reconfiguring the reservoir’s biophysical parameters is critical for high performance.

acquisition function. Given the best NRMSE value found so far, f_{\min} , the EI at a point \mathbf{x} is calculated as:

$$EI(\mathbf{x}) = (\mu(\mathbf{x}) - f_{\min})\Phi(Z) + \sigma(\mathbf{x})\phi(Z), \quad (6)$$

where $Z = (\mu(\mathbf{x}) - f_{\min})/\sigma(\mathbf{x})$.

Here, $\Phi(\cdot)$ and $\phi(\cdot)$ are the Cumulative Distribution Function (CDF) and Probability Density Function (PDF) of the standard normal distribution, respectively. The optimizer selects the next point to evaluate by finding the parameters that maximize this EI value: $\mathbf{x}_{\text{next}} = \arg \max_{\mathbf{x}} EI(\mathbf{x})$.

This formal approach allows us to efficiently navigate the vast parameter landscape and converge upon high-performing, task-specific configurations without the prohibitive cost of an exhaustive grid search.

III. RESULTS AND DISCUSSION

Our investigation, guided by Bayesian optimization, successfully identified distinct and robust operational regimes for the MC-PRC. These regimes are defined by clusters of biophysical parameters that optimize the reservoir for fundamentally different computational functions, analogous to the distinct material phases used for computation in other PRC systems [3]. We define two main regimes—memory-dominant and nonlinearity-dominant—and a third hybrid regime that balances both properties.

A. Defining Biophysical Computational Regimes

The Bayesian optimization process converged on different sets of biophysical parameters for each task class, confirming

that task-adaptability is not only possible but necessary. Table I summarizes the optimal parameter sets found for each of the three benchmark tasks for the deterministic model while Table II refers to the general trend of the top 10 Bayesian trials yielding the lowest NRMSE values from Fig. 2a.

TABLE I
OPTIMIZED BIOPHYSICAL PARAMETERS FOR EACH TASK REGIME

| Parameter | Forecasting (MG) | Transform. (Sine-Sq.) | Hybrid (MG-Cubed) |
|---|------------------------|------------------------|------------------------|
| NRMSE (Det.) | 0.097 | 0.237 | 0.307 |
| k_{on} ($\text{m}^3 \text{s}^{-1}$) | 6.64×10^{-19} | 1.55×10^{-17} | 2.47×10^{-18} |
| k_{off} (s^{-1}) | 4.15 | 2.78 | 2.31 |
| T (s) | 1.99 | 1.22 | 1.50 |
| d (μm) | 5.12 | 4.09 | 5.35 |
| N_{\max} | 19400 | 19925 | 11030 |
| D ($\text{m}^2 \text{s}^{-1}$) | 1.02×10^{-11} | 1.82×10^{-10} | 1.47×10^{-11} |

The Forecasting (Memory-Dominant) Regime, optimized for the Mackey-Glass task, is characterized by parameters that enhance the channel’s fading memory. As seen in Fig. 2a, this is achieved through a low D ($1.02 \times 10^{-11} \text{ m}^2 \text{s}^{-1}$), high N_{\max} (≈ 19400) and a long T (1.99 s), which together maximize ISI; allowing the reservoir to retain a rich history of past inputs.

The Transformation (Nonlinearity-Dominant) Regime, optimized for the sine-to-square task, favors parameters that promote a strong, rapid nonlinear response. This is achieved

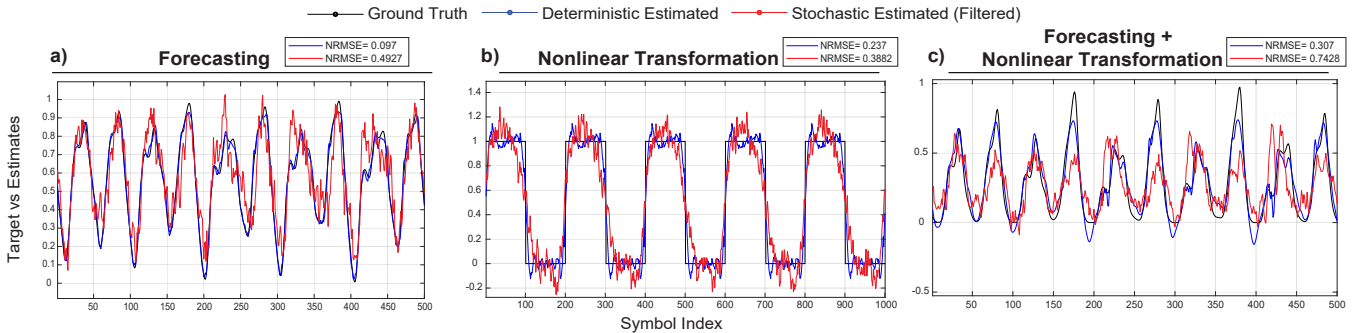


Fig. 3. Demonstration of task-adaptability through performance comparison on three distinct computational benchmarks [13]. Each plot shows the target ground truth (black), the prediction from the idealized deterministic model (blue), and the averaged prediction from three particle-based stochastic Smoldyn simulations with moving average window (red). The results for each task were generated using a unique set of biophysical parameters identified via Bayesian optimization. (a) Forecasting Task: On the memory-dominant Mackey-Glass time-series prediction with 6 symbols ahead, the deterministic achieved an NRMSE of 0.097 whereas filtered stochastic(Mov. Av. Window of 2000) achieved 0.4927. (b) Nonlinear Transformation Task: For the nonlinearity-dominant sine-to-square wave transformation, the deterministic achieved an NRMSE of 0.237 whereas filtered stochastic(Mov. Av. Window of 6000) achieved 0.3882. (c) Combination Task: The model also performs effectively on the Mackey-Glass Cubed task with 10 symbols ahead, which requires a balance of both memory and nonlinearity, the deterministic achieved an NRMSE of 0.307 whereas filtered stochastic(Mov. Av. Window of 2000) achieved 0.7428.

TABLE II
SUMMARY OF DISCOVERED BIOPHYSICAL REGIMES FOR COMPUTATIONAL TASKS

| Parameter | Forecasting (MG) | Transform. (Sine-Sq.) | Hybrid (MG-Cubed) |
|--|--------------------------------------|-----------------------------------|---------------------------|
| $k_{\text{on}} (\text{m}^3 \text{s}^{-1})$ | Very Low (10^{-19} – 10^{-18}) | High (10^{-17}) | Low (10^{-18}) |
| $k_{\text{off}} (\text{s}^{-1})$ | Mid-to-High | Mid-to-High | Low |
| $T (\text{s})$ | Long ($> 1.7 \text{s}$) | Short/Medium ($< 1.5 \text{s}$) | Long ($> 1.5 \text{s}$) |
| $d (\mu\text{m})$ | Mid (4–5) | Mid (4–5) | Mid (4–5) |
| N_{max} | High | High | Medium |
| $D (\text{m}^2 \text{s}^{-1})$ | Very Low (10^{-12} – 10^{-11}) | High (10^{-10}) | Very Low (10^{-11}) |

with a much higher D ($1.82 \times 10^{-10} \text{ m}^2 \text{s}^{-1}$), a shorter T (1.22 s), and a high N_{max} (≈ 19925) to drive the receiver into saturation, which is the source of the required nonlinearity.

The Hybrid Regime, optimized for the complex Mackey-Glass Cubed task, requires a balance of both memory and nonlinearity. The resulting parameters represent a compromise: memory is established via a mediocre T (1.50 s), largest distance (5.35 μm), and the lowest k_{off} (2.31s^{-1}), while the lower N_{max} (≈ 11030) prevents hard saturation that would otherwise destroy subtle temporal information.

The distinct nature of these operational profiles is visualized in Fig. 2a. While the three task-optimized regimes are clearly separated, the plot reveals that certain parameter values are significant for high performance across all tasks, such as a transmitter-receiver distance of approximately 4–5 μm and a memory window length near 5. However, for other parameters, clear trade-offs emerge. For instance, memory-intensive tasks (Forecasting, Hybrid) converge on a long symbol duration (T), while the Transformation task requires a significantly

shorter T . The most crucial finding relates to the binding affinity (K_{D}). Although a low K_{D} is beneficial in all tasks, the physical strategy to achieve it is task-dependent: the Transformation task leverages an extremely high association rate (k_{on}), whereas the Forecasting task relies on a very low dissociation rate (k_{off}). This demonstrates that peak performance is not achieved through a single set of “good” parameters, but through the fine-tuning of competing biophysical dynamics to meet specific computational demands.

B. Task-Specific Performance and Validation

The performance of the MC-PRC when configured with its task-optimized parameters is shown in Fig. 3. For the memory-dominant forecasting task (Fig. 3a), the deterministic model’s prediction (blue) closely tracks the ground truth (black), achieving a low NRMSE of 0.097. Similarly, the system excels at the nonlinearity-dominant transformation task (Fig. 3b), successfully converting the input sine wave into a square wave with an NRMSE of 0.237. The hybrid task (Fig. 3c) also shows effective performance with an NRMSE of 0.307, demonstrating the reservoir’s ability to balance both computational properties. In all cases, the filtered stochastic predictions (red) qualitatively reproduce the dynamics of the target signal, although, as expected, with a lower quantitative accuracy than the idealized deterministic model.

To validate the necessity of these distinct regimes, we performed a “criss-cross” validation experiment on the deterministic model, the results of which are shown in Fig. 2b. This experiment confirms that applying mismatched parameter sets leads to a degradation in performance, proving that reconfiguration of the reservoir is critical for optimal computation.

C. Impact of Stochasticity and Mitigation Strategies

While the deterministic model provides an idealized view, a realistic MC channel is subject to molecular noise from the stochastic nature of diffusion and binding. To create a more

physically realistic model, we validated our findings using the high-fidelity particle-based simulator, Smoldyn [15].

1) Hyperparameter Selection for Stochastic Simulations:

A direct one-to-one mapping of the optimal deterministic parameters to the stochastic simulator was not always feasible. Certain parameter combinations, particularly those involving extremely short distances, high numbers of molecules (N_{\max}), and very low diffusion coefficients (D), create computationally intractable scenarios for a particle-based simulator by generating an immense particle density in a small volume. Therefore, for each task, the hyperparameter set for the Smoldyn validation was selected from the top 10 best-performing candidates found by the Bayesian search, prioritizing physical realism and computational feasibility. The same set of parameters was then used for the final deterministic and stochastic comparisons shown in Fig. 3. Table I describes these parameters in detail.

2) *Mitigation of Molecular Noise via Causal Temporal Averaging*: The raw output from the stochastic simulations exhibited a tangible degradation in performance due to high-frequency molecular noise. To mitigate this, we implemented a causal moving average filter, a form of a Finite Impulse Response (FIR) low-pass filter, on the continuous-time signal of bound receptors, $s_{\text{raw}}(t)$, before the time-multiplexing step. The filtered signal, $s_{\text{filtered}}(t)$, is computed as:

$$s_{\text{filtered}}(t) = \frac{1}{W} \sum_{i=0}^{W-1} s_{\text{raw}}(t - i\Delta t) \quad (7)$$

where W is the averaging window size in samples and Δt is the simulation time step.

The optimal window size W was determined empirically for each task class. For the forecasting and hybrid tasks, a distinct performance optimum was found at $W = 2000$. For the transformation task, a larger window of $W = 6000$ was chosen at the point of diminishing returns, as it captured the vast majority of performance improvement. The filtering strategy significantly improved the NRMSE results.

IV. CONCLUSION

In this work, we have demonstrated that a canonical MC channel can be effectively repurposed as a task-adaptive PRC. By leveraging Bayesian optimization, we successfully navigated the high-dimensional biophysical parameter space to reconfigure the reservoir's dynamics, tailoring its computational properties for distinct tasks. Our findings reveal a fundamental trade-off: regimes with slow diffusion and ligand-receptor kinetics foster the long channel memory required for chaotic time-series forecasting, whereas regimes that promote faster, sharper receptor responses yield the nonlinearity essential for complex data transformations.

Our dual simulation approach confirms that this principle holds in both an idealized deterministic model and a stochastic system governed by molecular noise. While the inherent stochasticity in the particle-based model presents a challenge, we have shown that its impact can be partially mitigated through basic signal processing, affirming the viability of

this approach. The successful optimization of these disparate computational regimes *in silico* paves the way for a new class of unconventional computing hardware. Future work will focus on translating these findings into physical implementations, exploring methods for the online, dynamic tuning of parameters—for instance, by modulating receptor kinetics via allosteric modulators or altering diffusion via temperature control—to create truly adaptive “wetware” computing systems that can reconfigure their physical properties in real-time.

ACKNOWLEDGMENT

We thank Mustafa Uzun for foundational ideas and discussions, and Dr. Steve Andrews for Smoldyn and his generous technical guidance. This work was supported by The Scientific and Technological Research Council of Turkey (TUBITAK) under Grants #123E516 and #123C592.

RESOURCES

The authors have kept a record for codebase and data at <https://github.com/SYanon/mc-channels-reservoir-matlab.git>

REFERENCES

- [1] G. Tanaka, et al., “Recent advances in physical reservoir computing: A review,” *Neural Networks*, vol. 115, pp. 100-123, 2019.
- [2] S. Stepney, “Physical reservoir computing: a tutorial,” *Natural Computing*, pp. 1-21, 2024.
- [3] O. Lee, et al., “Task-adaptive physical reservoir computing,” *Nature Materials*, vol. 23, no. 1, pp. 79-87, Nov. 2023.
- [4] M. Uzun, K. B. Ikitz, and M. Kuscu, “Molecular Communication Channel as a Physical Reservoir Computer,” *arXiv preprint arXiv:2504.17022*, 2025.
- [5] M. Kuscu, E. Dinc, B. A. Bilgin, H. Ramezani, and O. B. Akan, “Transmitter and Receiver Architectures for Molecular Communications: A Survey on Physical Design with Modulation, Coding, and Detection Techniques,” *Proc. IEEE*, vol. 107, no. 7, pp. 1302-1341, 2019.
- [6] H. Jaeger and H. Haas, “Harnessing nonlinearity: Predicting chaotic systems and saving energy in wireless communication,” *Science*, vol. 304, no. 5667, pp. 78-80, 2004.
- [7] S. Shahi, F. H. Fenton, and E. M. Cherry, “Prediction of chaotic time series using recurrent neural networks and reservoir computing techniques: A comparative study,” *Machine learning with applications*, vol. 8, p. 100300, 2022.
- [8] M. Kuscu, “Adaptive Molecular Communication Receivers with Tunable Ligand-Receptor Interactions,” *arXiv preprint arXiv:2305.06481*, 2023.
- [9] V. Jamali, et al., “Channel modeling for diffusive molecular communication—A tutorial review,” *Proc. IEEE*, vol. 107, no. 7, pp. 1256-1301, 2019.
- [10] J. Snoek, H. Larochelle, and R. P. Adams, “Practical Bayesian Optimization of Machine Learning Algorithms,” in *Proc. Neural Information Processing Systems (NIPS)*, 2012.
- [11] M. Pierobon and I. F. Akyildiz, “Noise analysis in ligand-binding reception for molecular communication in nanonetworks,” *IEEE Transactions on Signal Processing*, vol. 59, no. 9, pp. 4168-4182, 2011.
- [12] H. Jaeger, “The “echo state” approach to analysing and training recurrent neural networks,” *GMD Technical Report*, vol. 148, 2001.
- [13] C. Wringe, M. Trefzer, and S. Stepney, “Reservoir computing benchmarks: a tutorial review and critique,” *International Journal of Parallel, Emergent and Distributed Systems*, pp. 1-39, Mar. 2025.
- [14] M. Mendula, M. Miozzo, and P. Dini, “Reservoir Computing in Real-World Environments: Optimizing the Cost of Offline and Online Training,” *TechRxiv*, May 2025. [Online]. Available: <https://doi.org/10.36227/techrxiv.174742037.78551676/v1>
- [15] S. S. Andrews, “Smoldyn: Particle-based simulation with rule-based modeling, improved molecular interaction and a library interface,” *Bioinformatics*, vol. 33, no. 5, pp. 710-717, 2017.